Cancer Cell
Article

NEK2 Induces Drug Resistance Mainly through Activation of Efflux Drug Pumps and Is Associated with Poor Prognosis in Myeloma and Other Cancers

Wen Zhou,[1,3,6] Ye Yang,[1,3,6] Jiliang Xia,[1,3,6] He Wang,[1,3,6] Mohamed E. Salama,[2] Wei Xiong,[3] Hongwei Xu,[1,3] Shashirekha Shetty,[4] Tiehua Chen,[3] Zhaoyang Zeng,[3] Lei Shi,[3] Maurizio Zangari,[3] Rodney Miles,[2] David Bearss,[5] Guido Tricot,[1,*] and Fenghuang Zhan[1,3,*]

[1]Division of Hematology, Oncology, and Blood and Marrow Transplantation, Department of Internal Medicine, University of Iowa, Iowa City, IA 52242, USA
[2]Department of Pathology, University of Utah and ARUP Lab, 500 Chipeta Way, Salt Lake City, UT 84108, USA
[3]Division of Hematology, University of Utah School of Medicine, 30 North 1900 East, Salt Lake City, UT 84132, USA
[4]Cleveland Clinic, 9500 Euclid Avenue, Mail Code LL2-2, Cleveland, OH 44195, USA
[5]Physiology and Developmental Biology 471 WIDB, Brigham Young University, Provo, UT 84602, USA
[6]These authors contributed equally to this work
*Correspondence: guido-tricot@uiowa.edu (G.T.), fenghuang-zhan@uiowa.edu (F.Z.)
http://dx.doi.org/10.1016/j.ccr.2012.12.001

SUMMARY

Using sequential gene expression profiling (GEP) samples, we defined a major functional group related to drug resistance that contains chromosomal instability (CIN) genes. One CIN gene in particular, *NEK2*, was highly correlated with drug resistance, rapid relapse, and poor outcome in multiple cancers. Overexpressing *NEK2* in cancer cells resulted in enhanced CIN, cell proliferation and drug resistance, while targeting *NEK2* by NEK2 shRNA overcame cancer cell drug resistance and induced apoptosis in vitro and in a xenograft myeloma mouse model. High expression of NEK2 induced drug resistance mainly through activation of the efflux pumps. Thus, *NEK2* represents a strong predictor for drug resistance and poor prognosis in cancer and could be an important target for cancer therapy.

INTRODUCTION

Multiple myeloma (MM) is the second most common hematologic malignancy, and affects over 20,000 patients each year in the United States, with nearly 11,000 deaths during the same time period (Jemal et al., 2009). A major reason for cancer treatment failure is the existence of a drug-resistant subclone, either present at diagnosis or developed during treatment. To achieve a cure for myeloma, a better understanding of the genetic makeup of these drug-resistant myeloma cells is required so that these cells can be specifically targeted.

Traditional prognostic factors such as β2-microglobulin, albumin, and C-reactive protein account for at most 15%–20% of the heterogeneity in outcomes. Currently, the best marker for incurable myeloma is the presence of abnormal metaphase cytogenetics, but even its prognostic value is limited because its presence accounts for less than 30% of the observed variability in outcome of newly diagnosed patients (Calasanz et al., 1997). Using molecular genetic tools, such as FISH analysis, many of the partners involved in translocations with 14q32 (heavy chain gene locus) in myeloma have been identified (Avet-Loiseau et al., 2002). These include t(4;14) involving *FGFR3/MMSET*, t(14;16) involving *c-MAF*, and t(14;20) involving *MAF-B*. These translocations are correlated with poor prognosis and are very often associated with chromosome 13 deletion on metaphase cytogenetics (Moreau et al., 2002). Large sample FISH studies also identified that 17p13 (p53 gene locus) deletion was a poor prognostic indicator (Xiong et al., 2008). Furthermore, global gene expression profiling (GEP) has emerged as a powerful tool to classify

Significance

Drug resistance is a universal problem with current cancer therapies. We demonstrate that overexpression of CIN genes, especially *NEK2*, and drug resistance are closely correlated and lead to a poor outcome in myeloma and other cancers. Furthermore, targeting *NEK2* can overcome drug resistance and inhibit cancer cell growth in vitro and in vivo. Our findings have the potential to translate into very important prognostic and therapeutic clinical tools. Overexpression of NEK2 has been shown to be associated with aggressive cancer behavior and poor prognosis in many malignancies and, therefore, our findings should also apply to other hematologic malignancies and solid tumors.

disease subtypes, to develop robust prognostic models, and to identify new drug resistance-associated targets in cancers (Shipp et al., 2002). Based on GEP, we and others have identified a 70 high-risk gene model and molecular and genetic myeloma subgroups that are linked to patient outcome (Bergsagel et al., 2005; Shaughnessy et al., 2007). Because GEP data can be obtained repeatedly over time, we hypothesize that it is possible to monitor, during therapy, genetic changes associated with the emergence of a drug-resistant cancer cell population. We therefore performed sequential GEPs to define a myeloma transcriptome either after chemotherapy or at relapse occurring early after treatment (early relapse) indicative of a drug-resistant tumor subpopulation.

Our goal in this study is to identify a reliable, clinically useful prognostic gene expression signature that offers clinical opportunities for predicting drug resistance and developing treatments in myeloma and other cancers. We also determine the effects of NEK2 overexpression on disease progression and drug resistance and explore how high expression of NEK2 induces drug resistance in cancer cells.

RESULTS

Sequential Analyses of Gene Expression Profiling Reveal a Chromosomal Instability Signature Associated with Myeloma Drug Resistance and Early Disease Relapse

We compared GEP of 19 paired myeloma cell samples collected at diagnosis and again after induction chemotherapy (before first stem cell transplant). A total of 615 probe sets displayed significant differential expression. Similarly, we compared the GEP of 51 paired myeloma samples collected at baseline and at early relapse and found 864 differentially expressed genes. By intersection analyses of these two comparisons, we identified 56 common genes with significantly upregulated expression both after chemotherapy and at relapse (Figures 1A and 1B; Table S1 available online). The major functional group including ten genes (*TOP2A*, *CDC20*, *TRIP13*, *NEK2*, *AURKA*, *RRM2*, *CCNB1*, *KIF4A*, *CEP55*, and *PBK*), with a significant negative impact on survival (hazard ratio [HR] $\geq$ 2), belongs to the well-established chromosomal instability (CIN) signature (Carter et al., 2006). Importantly, serial GEPs obtained pre-first, pre-second, and post-second autologous stem cell transplants (ASCT) showed either a continuing increase of CIN signature or a stable high level of CIN signature (Figure 1C). Supervised clustering using these ten CIN genes was applied to plasma cells from 22 healthy donors, 44 patients with monoclonal gammopathy of undetermined significance (MGUS), 351 patients with newly diagnosed MM, and nine human myeloma cell lines. Results revealed that a small population of patients with newly diagnosed MM (~10%) showed a pattern with very high expression levels of this CIN signature, similar to that of MM cell lines (which are derived from terminal MM patients) (Figure 1D). The mean expression levels of CIN genes defined a high-risk score associated with significantly shorter duration of response, of event-free survival (EFS) (Figure 1E, $p < 0.001$; HR = 4.6), and of overall survival (OS) (Figure 1F: $p < 0.001$; HR = 5.2).

NEK2, a CIN Gene, Is Linked to Poor Survival in MM and Other Cancers

Since drug resistance is associated with poor prognosis, we also correlated the gene expression of the 56 genes associated with drug resistance with clinical outcomes. A Kaplan-Meier survival analysis was performed on the Total Therapy 2 (TT2) cohort, which included 668 patients with newly diagnosed myeloma, and available GEP on the last 351 patients enrolled (Barlogie et al., 2006). The correlation between gene expression and survival was determined by the p value and HR at the best expression signal cut-off using R-package. *NEK2* was the gene most strongly associated with inferior survival in unadjusted log rank tests (Table S1).

As shown in Figure 2, the top 13% of MM patients with the highest *NEK2* expression had a significantly inferior EFS, OS (Figures 2A and 2B, both $p \leq 0.0001$), and postrelapse survival in TT2 (Figure 2C, $p < 0.0001$), as well as in the successor study TT3 (Figures 2D and 2E, $p < 0.0001$ and $p = 0.0015$, respectively). On correlation analyses of clinical characteristics, *NEK2* gene expression represented an independent factor associated with poor prognosis in TT2 (Table 1). Patients with high *NEK2* expression level had high levels of creatinine ($p = 0.012$) and lactate dehydrogenase (LDH) ($p = 0.004$), and low levels of albumin ($p = 0.018$); an increased frequency of hypodiploidy defined by metaphase cytogenetic analysis ($p < 0.001$), of deletion of chromosome 13 by metaphase analysis ($p = 0.001$), of amplification of 1q21 by FISH analysis ($p < 0.001$); and increased numbers of focal myeloma bone lesions on magnetic resonance imaging ($p = 0.010$). Similarly, the high-risk group defined by the 70-gene model, and the clinically more aggressive subgroups of the *MMSET/FGFR3, MAF/MAFB*, and *Proliferation* (*PR*) predominated in the high *NEK2* cohort ($p < 0.001$). On multivariate cox regression analysis, high *NEK2* expression independently conferred inferior OS (Table 1, $p = 0.032$).

To examine the clinical implication of high *NEK2* expression in other cancers, we used microarray data sets and associated clinical information of seven different cancers, including acute myeloid leukemia (Figure S1A), bladder cancer (Figure S1B), breast cancer (Figure S1C), glioma (Figure S1D), lung adenocarcinoma (Figure S1E), mantle cell lymphoma (Figure S1F), and mesothelioma (Figure S1G). We found that overexpression of *NEK2* conferred an inferior survival in all seven cancers (Figures S1A–S1G, $p < 0.0001$). *NEK2* expression was also significantly upregulated compared to normal cells in all of the examined cancers, including head and neck squamous cell carcinoma (Figure S1H), bladder carcinoma (Figure S1I), glioblastoma (Figure S1J), T cell acute lymphoblastic leukemia (Figure S1K), colon carcinoma (Figure S1L), hepatocellular carcinoma (Figure S1M), melanoma (Figure S1N), and ovarian adenocarcinoma (Figure S1O).

Increased NEK2 Expression Induces Drug Resistance, Cell Proliferation, and Chromosomal Instability in Cancer

To test the functional role of *NEK2*, we overexpressed NEK2 by lentivirus-mediated NEK2-cDNA transfection in normal fibroblasts BJ; the MM cell lines ARP1, KMS28PE, and OCI-MY5; the lung cancer cell line H1299; and the breast cancer cell line MCF7 (Figure 3A). NEK2 overexpression significantly

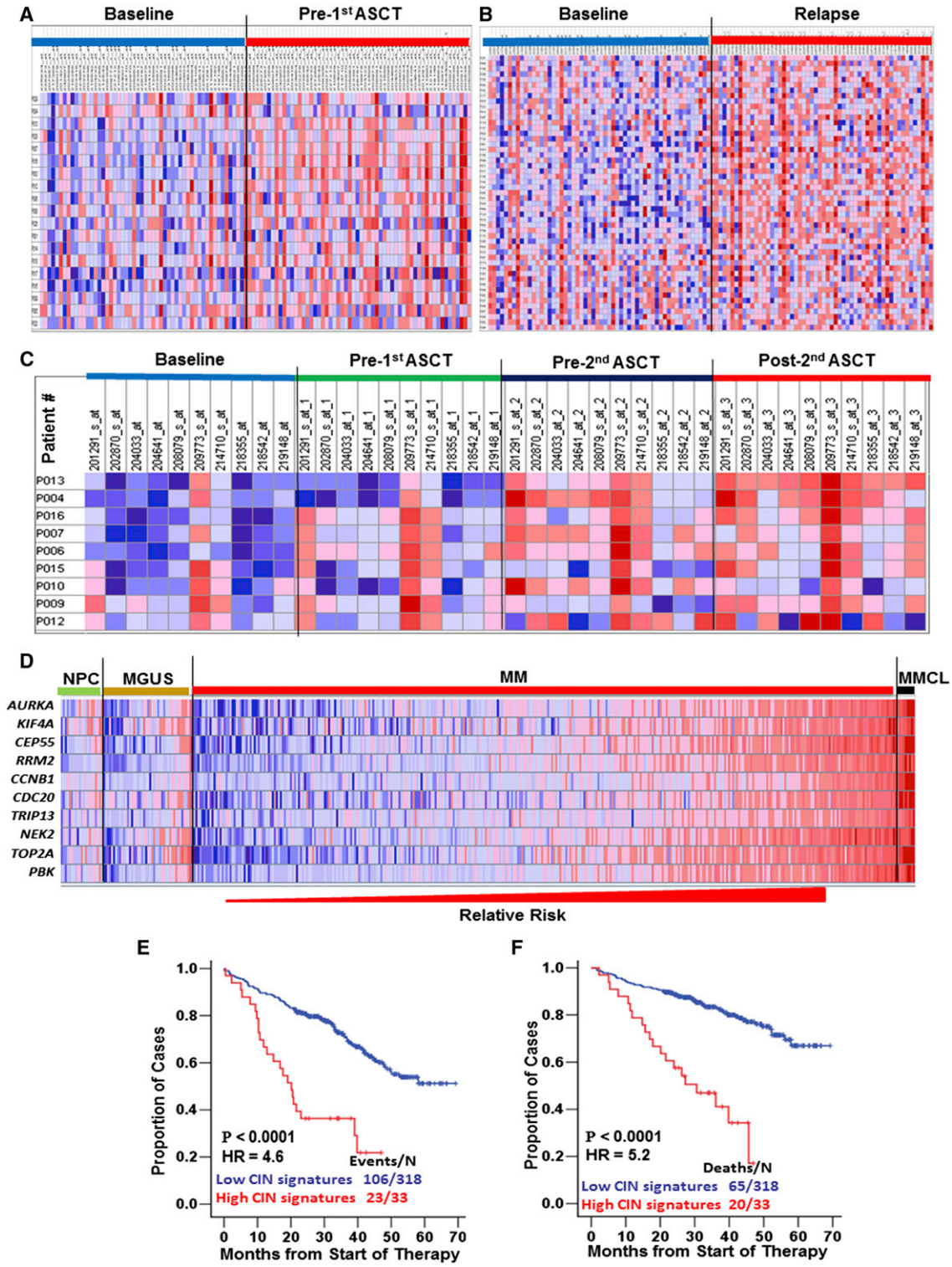

Figure 1. Identification of Genes Related to Myeloma Drug Resistance and Disease Relapse

(A and B) Heat maps of the 56 differentially expressed genes in paired myeloma samples at baseline and either after chemotherapy (n = 19) (A) or at relapse (n = 51) (B). Patient samples were plotted on the vertical axis and the gene probe sets were listed on top along the horizontal axis. See also Table S1.

(C) A complete sample set (at diagnosis, pre-first, pre-second, and post-second transplants) was available for nine of the 19 patients. The expression of CIN genes increased significantly in myeloma cells during chemotherapy, suggesting a strong relationship with drug resistance. Red color for a gene indicates expression above the median and blue color indicates expression below the median.

(legend continued on next page)

increased cell proliferation in both normal and cancer cells compared with empty vector (EV)-transfected cells (Figures 3B and 3C).

To examine the effect of *NEK2* on cancer cell growth and drug resistance, a clonogenic soft agar assay was performed using NEK2 overexpressing MM cell line ARP1 and lung cancer cell line H1299 treated with different doses of anticancer drugs: bortezomib, doxorubicin, or etoposide. Similar results for these two cell lines were obtained. Results from the representative ARP1 group are shown in Figure 3D. Cancer cells overexpressing NEK2 showed a significant increase in colony formation indicating that high levels of NEK2 promote cancer cell proliferation (Figure 3D, $p < 0.05$). Furthermore, compared with nontreated controls, cancer cells overexpressing NEK2 showed only a slight decrease in their capacity to form colonies for all three drugs tested at a low dose (Figure 3D). However, control cells transfected with EV showed a significant decrease in colony formation when incubated with these drugs at the same concentrations. To answer whether *NEK2* conferred drug resistance is associated with decreased apoptosis, the standard apoptosis assay was performed on the same two cell lines after treatment with the same drugs for 48 hr. Apoptotic cells were stained by the APC-conjugated Annexin-V and determined by flow cytometry. As shown in Figure 3E, overexpression of NEK2 decreases cell apoptosis after addition of anticancer drugs compared with controls.

To determine the correlation between NEK2 expression and cell proliferation, we performed Ki67 immunostaining on 32 primary myeloma cases. Double staining for CD138 and Ki67 was used to identify the myeloma cells. Overall, we observed a low proliferation index in myeloma cells (Figures 3F and 3H). NEK2 immunostaining was performed on 26 newly diagnosed cases. Cells were scored positive for NEK2 if they showed nuclear expression (Figures 3G and 3I). No significant correlation was noted between Ki67 and NEK2 expression ($p > 0.05$). We further correlated the gene proliferation index (GPI) (Hose et al., 2011) with *NEK2* expression in the 351 TT2 patients with newly diagnosed myeloma. A high correlation was found between the GPI50 and NEK2 signal (data not shown; $r = 0.83$, $p < 0.001$). We also found that the predictive value for patient outcome of *NEK2* alone was as high as of that of the GPI 50 genes (Figure S2). To determine whether the increased *NEK2* signature in post-treatment samples especially post-second ASCT is due to contamination with other nonmyeloma cells, we stained bone marrow samples from nine post-second ASCT patients, who were in complete remission (CR), using double staining for CD138 and NEK2. Increased NEK2 expression in CD138 positive plasma cells (>50%) was noted in five of nine cases. Expression of NEK2 was significantly higher in myeloma cells when compared to other hematopoietic cells (Figures 3J and 3K). NEK2 protein was noted in minority of normal hematopoietic cells but much weaker than in the myeloma cells.

To explore if high expression of *NEK2* can induce chromosomal instability, we subsequently performed comparative genomic hybridization (CGH)-array using cell lines transfected with NEK2 versus wild-type (WT) cell lines, and cell lines transfected with EV versus WT cell lines. Exactly the same generation of ARP1 and H1299 cell lines was transfected with NEK2 and EV and used to compare with the same generation of parental cells (WT). The log2 ratio for each probe was displayed on the vertical axis, and the probe's genomic location on the horizontal axis (Figures 4A, 4B, 4E, and 4F). We identified gains and losses of multiple segments in the NEK2 overexpressing ARP1 and H1299 but not in the cells transfected with EV. We chose the chromosomes 4q21 and 21q22 as examples in Figures 4C and 4G and showed DNA losses in these areas for ARP1 and H1299, respectively. To verify the array-CGH findings, we subsequently performed FISH analysis using probes of areas deleted by array-CGH on ARP1 cells (probes 4q21.23 in green) and showed four, four, and three copies, respectively in the WT, EV, and NEK2 cells (Figure 4D). Probe 21q22 (LSI21 in red) showed five, five, and two copies in the H1299 WT, EV, and NEK2 cells (Figure 4H), respectively. However, control FISH probes chosen from random segments of each cell line, which did not show gain or loss by array-CGH, also did not show a difference in copy number by FISH analysis.

Knockdown of NEK2 by shRNA Inhibits Myeloma Cell Growth and Decreases Drug Resistance In Vitro and in NOD-Rag/null Gamma Mice

To examine the function of *NEK2* in promoting cancer cell survival, four specific shRNAs against *NEK2* gene (sh1-4) were designed. A tetracycline-inducible lentiviral expression system containing shRNA to NEK2 was used to knockdown NEK2 in tumor cells; sh1-3 target the *NEK2* coding region and sh4 targets the 3′ untranslated region (UTR). Real-time PCR confirmed a remarkable downregulation of *NEK2* expression in ARP1 MM cells after transfection of these NEK2-shRNAs, especially sh3 (Figure S3A). NEK2-shRNA-induced growth inhibition and cell death were examined daily. Cells were cultured for 6 days and nontarget scramble-transfected cells were used as controls. As shown in Figures S3B and S3C, all four NEK2-shRNAs significantly induced growth inhibition (Figure S3B) and cell death (Figure S3C) compared with the scrambled controls. To address the issue of off-target toxicities, we doubly transfected ARP1 cells with NEK2-sh4 and the NEK2-cDNA, which contained only the coding region of *NEK2*, and cell growth was examined. As shown in Figure S3D, forced overexpression of NEK2 in ARP1 cells successfully abrogated cell growth inhibition induced by sh4, strongly suggesting that the cytotoxic effects induced by sh4 were directly related to specific knockdown of NEK2. We then chose the most potent NEK2-sh3 to knockdown NEK2 in other cancer cell lines, including KMS28PE, OCI-MY5, H1299, and MCF7 cells. Figures 5A and 5B confirm that NEK2-knockdown

(D) Gene expression clustergram of 10 CIN genes in plasma cells from 22 healthy subjects (NPC), 44 subjects with MGUS, 351 patients with newly diagnosed MM, and nine human MM cell lines (MMCL). Samples within myeloma risk groups were ordered so that the predicted risk increases continuously from left to right.
(E and F) Kaplan-Meier analyses showed that the top 10% of uniformly-treated MM patients with high CIN signatures had a significantly inferior EFS (E) and OS (F).

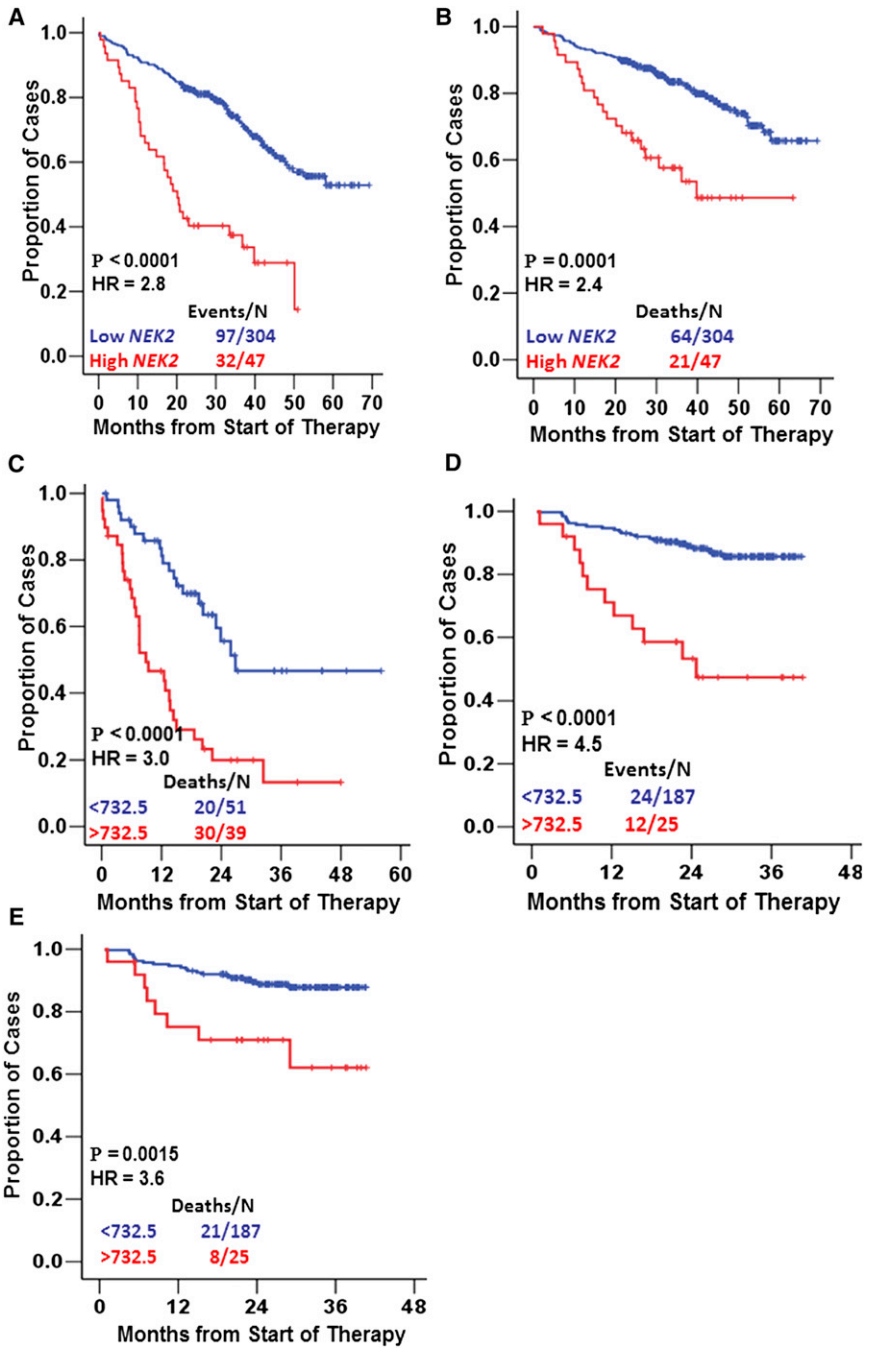

Figure 2. High NEK2 Expression Is Linked to a Poor Prognosis in Myeloma

(A and B) Kaplan-Meier analyses of EFS (A) and OS (B) revealed inferior outcomes among the 47 patients with NEK2 high expression compared with the remaining 304 patients with NEK2 low-expression in the TT2 trial.

(C) Kaplan-Meier analysis of post-relapse survival was shown in relation to NEK2 expression determined by GEP. High expression of NEK2 conferred a short post-relapse survival.

(D and E) Kaplan-Meier analyses of EFS (D) and OS (E) revealed an inferior outcome among the 25 patients with NEK2 high-expression compared with the remaining 187 patients with NEK2 low-expression in our TT3 trial.

See also Figure S1.

induced significant cell growth inhibition and apoptosis in all these cell lines compared with the scrambled controls. Western blots confirmed efficient knockdown of NEK2 in these cells (Figure 5C).

To examine the mechanism by which NEK2-knockdown induced cell death, NEK2-silenced ARP1, KMS28PE, OCI-MY5, H1299, and MCF7 cells were cultured for 3 days. As shown in Figure 5C, increased levels of cleaved PARP, and activation of caspase-3, caspase-8, and caspase-9 were observed by the appearance of the processed forms on western blots in NEK2-knockdown cancer cells compared with scrambled cells, indicating that both death receptor-dependent (caspase 8) and -independent (caspase 9) apoptotic pathways were involved.

We also tested the effects of conditional knockdown of NEK2 on MM cell growth in vivo. In this study (5 mice in each group), ARP1 MM cells were transduced with NEK2-shRNA or scrambled RNA vectors and then injected subcutaneously into the right abdomen of NOD-Rag/null gamma mice. Ten days after engraftment of the tumors, viral expression was induced by the addition of doxycycline to the drinking water. As shown in Figure 5D, tumor cells in control mice continued to grow rapidly while activation of NEK2 shRNA, validated by downregulation of NEK2 on western blot (Figure 5F), resulted in a marked inhibition of tumor growth and decrease in tumor volume (Figure 5E).

We subsequently tested if downregulation of NEK2 expression could decrease drug resistance to bortezomib using the bortezomib-resistant (DR) ARP1 cell line. Viral expression was induced by the addition of doxycycline to the drinking water 15 days after the injection of tumor cells (three mice in each group). Bortezomib was given by intraperitoneal injection at the time the tumor could be palpated under the skin. The upper panel of Figure 5G shows similar tumor sizes after 15 days in one representative mouse from each group. We found that knockdown of NEK2 could inhibit tumor growth (the bottom panel of Figure 5G, group 3 versus group 1, and Figure 5H) and that bortezomib could further inhibit tumor growth only in tumors with downregulated NEK2 (Figures 5G, group 4 versus group 3, and 5H) but not in tumors with high levels of NEK2 (Figures 5G, group 1 versus group 2, and 5H). Western blots confirmed that NEK2 expression was indeed

Table 1. The Correlation of NEK2 Expression and Clinical Characteristics in TT2

Characteristics	High NEK2 (%, n = 47)	Low NEK2 (%, n = 304)	p Value
Age at least 65 years	19.6	22.3	NS
Female sex	39.1	43.9	NS
White race	95.7	87.5	NS
IgA isotype	30.4	27.5	NS
CRP at least 4.0 mg/l	11.1	5.3	NS
β2-Microglobulin at least 4.0 mg/l	45.7	32.8	NS
Hemoglobin less than 10 g/dl	34.1	24.0	NS
Bone marrow plasma cells (by aspiration) 33% or greater	48.6	53.2	NS
Albumin less than 3.5 g/dl	52.5	34.1	0.018
Creatinine at least 2.0 mg/dl (221 μmol/l)	22.7	9.8	0.012
MRI focal bone lesions, at least three	76.1	55.8	0.010
LDH at least 190 IU/l	53.3	31.3	0.004
Chromosomal abnormalities (by G-banding)	65.2	30.8	<0.001
Hyperdiploid	21.7	18.0	NS
Hypodiploid	43.5	11.1	<0.001
Deletion of chromosome 13	72.1	46.1	0.001
Amplification of 1q21	85.0	37.6	<0.001
High-risk model (70-gene) [a]	58.7	6.2	<0.001
Subgroups with poor prognosis (PR/MS/MF)[a]	82.6	18.4	<0.001
Multivariate Analysis of Clinical Characteristics Affecting OS[b]			
NEK2 high 13%			0.032
High-risk model (70-gene)[a]			0.001
Subgroups with poor prognosis (PR/MS/MF)[a]			0.040

[a]The high-risk model (Shaughnessy et al., 2007) and PR/MS/MF subgroup (Zhan et al., 2006) designation has been described elsewhere.
[b]Predictors with p > 0.05 for OS outcome: aged 65 years or older, IgA isotype, metaphase cytogenetic abnormalities, albumin of 35 g/l or less, β2 microglobulin 4 mg/l or above, LDH 190 IU/l or above, creatinine at least 2 mg/dl (221 μmol/l), bone marrow plasma cells (by aspiration) 33% or greater, and C-reactive protein of 4 mg/l or more.

downregulated by the addition of doxycycline in the ARP1-DR cells (Figure 5I).

Overexpression of NEK2 Activates both AKT and Canonical Wnt Signaling, Resulting in Increased Cancer Cell Proliferation, Drug Resistance, and Chromosomal Instability

NEK2 regulates the mitotic centrosome separation through reversible phosphorylation of its substrates c-NAP1 (Fry et al., 1998), protein phosphatase 1 (PP1) (Helps et al., 2000), NIP1/centrobin (Sonn et al., 2009), β-catenin (Bahmanyar et al., 2008), and SGO1 (Fu et al., 2007) in yeast. In our study, we performed co-immunoprecipitation (CO-IP) and mass spectrometry in cancer cells to identify NEK2 binding proteins. We found that NEK2 directly binds to PP1, mitotic arrest deficient 2 (MAD2), cell division cycle protein 20 (CDC20), β-catenin, highly expressed protein in cancer (HEC1), and protein regulator cytokinesis 1 (PRC1) (data not shown). We were particularly interested in PP1, β-catenin, CDC20, and MAD2, because they are involved not only in chromosomal instability, but also in cancer cell drug resistance and proliferation (Figure S4A). Western blots were applied to further elucidate the activation of the key signaling pathways related to drug resistance and anti-apoptosis, including PP1 and β-catenin. As shown in Figure 6A, overexpression of NEK2 not only phosphorylated PP1 at Thr-320 resulting in inhibition of PP1 activity (Kwon et al., 1997), but also activated canonical Wnt signaling evidenced by nuclear accumulation of β-catenin. We also examined two main mechanisms related to drug resistance, the efflux pumps and the mitotic checkpoint proteins, to see if increased expression of these proteins is associated with overexpression of NEK2 or its targets. Our studies showed that overexpression of NEK2 upregulated mitotic checkpoint protein MAD2 and ABC transporter family members, including ABCB1 (p-glycoprotein, MDR1), the multidrug resistance protein ABCC1 (MRP1), and the breast cancer resistant protein ABCG2 (BCRP) (Figure 6A). Consistently, downregulation of NEK2 by shRNA decreased the expression of phosplorylated PP1, AKT, nuclear β-catenin, and ABC transporters (Figure 6B). High expression of NEK2 promoted a higher efflux of the hydrophilic eFluxx-ID gold fluorescent dye from cancer cells compared with control cells (Figure 6C). Verapamil, an ABC transporter inhibitor, was able to abrogate part of the *NEK2*-induced drug resistance by showing a decrease in colony formation (Figure 6D). These results strongly suggest that PP1, Wnt, mitotic checkpoint proteins, and ABC transporter family signaling pathways are the downstream targets of NEK2.

It has indeed been confirmed that PP1 regulates the AKT signaling transduction pathway to control cell survival and differentiation (Xiao et al., 2010), and that this pathway plays a central role in cell proliferation and drug resistance. We observed a high correlation between deactivation of PP1 (increase of phosphorylated PP1 at Thr-320) and the activation of AKT pathways (Figure 6A). We thus determined the functional role of AKT pathway in *NEK2* inducing cell proliferation and drug resistance. A specific AKT inhibitor, LY294002, at the dose of 10 μM for 12 hr was used to treat NEK2-transfected ARP1 cells. LY294002 treatment decreased p-AKT in both EV - and NEK2-transfected myeloma cells compared with untreated controls on western blot (Figure 6E), confirming its specificity. LY294002 inhibited the ABC transporters *ABCB1*, *ABCC1*, and *ABCG2* in ARP1 NEK2-OE cells (Figure 6E). LY294002 inhibited to efflux of hydrophilic eFluxx-ID gold fluorescent dye in ARP1 NEK2-OE cells further supporting that AKT regulates the activity of ABC family (Figure 6F) and decreased colony formation in ARP1 NEK2-OE cells (Figure 6G).

Activation of Wnt signaling induces cancer cell survival and drug resistance (Gehrke et al., 2009). We have shown that NEK2 stabilized nuclear β-catenin (Figure 6A). We have further demonstrated the functional role of canonical Wnt signaling in *NEK2* induced cancer cell proliferation and drug resistance. Similar to the effect induced by the AKT inhibitor, knockdown

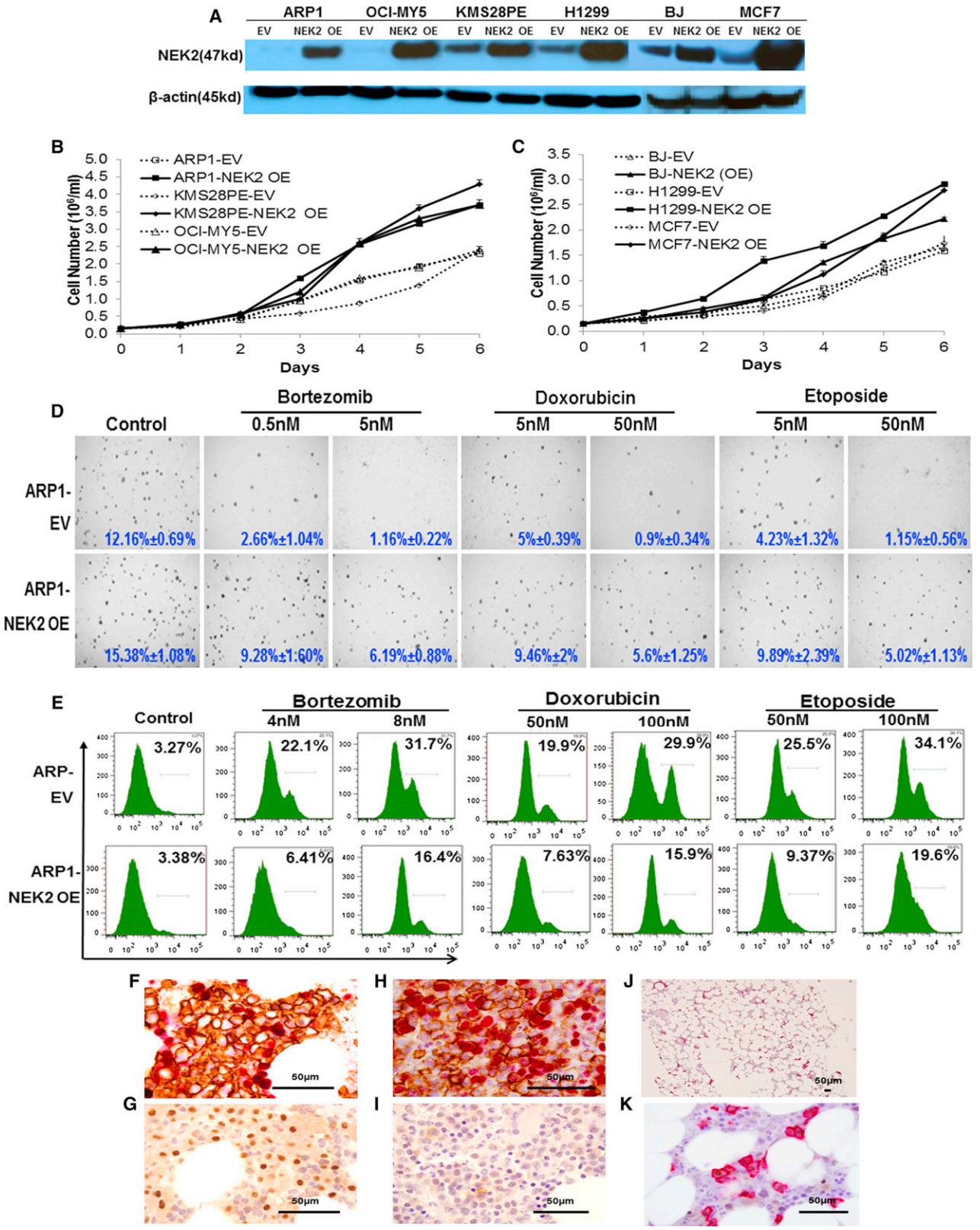

Figure 3. Overexpression of NEK2 Promotes Cancer Cell Proliferation and Drug Resistance

(A) Western blots showed increased NEK2 expression in the cancer cell lines ARP1, KMS28PE, OCI-MY5, H1299, and MCF7, and normal fibroblasts BJ after transfection with NEK2-cDNA. EV-transfected cells served as controls.

(legend continued on next page)

of β-catenin in NEK2-transfected ARP1 also abrogated drug resistance induced by *NEK2* (Figure 6G). Interestingly, the AKT inhibitor LY294002 decreased the nuclear accumulation of β-catenin in ARP1 NEK2-OE cells, suggesting that activation of Wnt signaling induced by *NEK2* partially depends on AKT pathway partially (Figure 6E).

In addition, we found that overexpression of NEK2 suppressed the expression of the pro-apoptotic genes BAD and PUMA and upregulated the expression of pro-survival genes BCL-xL and MCL-1, indicating a possible role of *NEK2* in anti-apoptosis (Figure S4B). Finally, the *NEK2* cell signaling related genes were analyzed by using GEP. It is noteworthy that the 76 probe sets related to either overexpressing or silencing NEK2 have a defined function in DNA replication, cell cycle progression, chromosome condensation, mitosis, and cytokinesis (*TMPO*, *MYBL1*, *HMGB1*, *HPSE*, *CDC2*, *KLF14*, *DUSP4*, *MPHOSPH9*, *PRKDC*, *CENPF*, *KLF11*, *CDCA2*, and *KIFC1*) (Figures S4C–S4F; Table S2).

DISCUSSION

Ron Morris first described NIMA in 1975 (Morris, 1975). The NIMA-related family members of serine/threonine kinases (Neks) are widespread among eukaryotes and are defined by similarities in their N-terminal catalytic domains to the founding NIMA member (Oakley and Morris, 1983). Together with the Polo and Aurora kinase families, the NIMA-related protein kinases (Nrks or Neks) have been called the third family of mitotic kinases (Wu et al., 1998). *NEK2*, a member of the NIMA-related family, has several putative roles in cell division, most notably in spindle formation and chromosome segregation (Faragher and Fry, 2003). Overexpression of active NEK2 leads to CIN and an aneuploid karyotype (Hayward and Fry, 2006), which are commonly observed in cancers including virtually all myelomas. Recently, it has been proposed that an increased number of chromosome sets can promote cell transformation and give rise to an aneuploid tumor (Storchova and Kuffer, 2008). In our study, we have demonstrated that overexpression of NEK2 induced chromosomal instability in cancer evidenced by multiple segment gains and losses of chromosome. Our results also demonstrated that the transcriptional level of *NEK2* is increased in many aggressive types of cancer. Using the publicly available data sets, we analyzed *NEK2* expression data from a large set of different primary and metastatic tumors with their normal counterparts serving as controls. In all cancers, we showed that regardless of the tissue of origin, tumor cells have significantly increased *NEK2* expression. Gene expression-based survival prediction in multiple independent cancers showed that overexpression of *NEK2* is associated with a poor clinical outcome. All these findings support the important role of the *NEK2* gene in disease progression not only in MM, but also in multiple other tumors. When we performed a multivariate analysis (MVA) with four parameters including the high-risk model (70 genes), high-risk genetics (MF, MS, PR), GPI50, and *NEK2*, only the high-risk 70-gene model and the high-risk genetics, but not GPI50 and *NEK2*, were significantly independent parameters in the prediction of MM prognosis (data not shown). This may be because *NEK2* is one of the GPI50 genes and its expression is highly correlated with the high-risk scores of both the 70-gene model and high-risk genetics. However, as shown in Table 1, high expression of *NEK2* is an independent prognostic factor in a MVA without GPI50 parameter.

Drug resistance is the most important problem in cancer treatment. Relapse phenotypes may be acquired via therapy-induced selection of resistant minor clones present at diagnosis or by direct adaptation to therapy of the original clone. Applying GEP, our study focused on identifying the genetic make-up of drug-resistant myeloma cells, which is very different from that of myeloma cells at diagnosis, when most myeloma cells are drug-sensitive. In this study, we defined 56 genes associated with drug-resistant myeloma cells, which either survive intensive treatments or are present in relapse, occurring early during treatment. A subset of ten genes, previously related to drug resistance, belong to the well-established chromosomal instability signatures. A prominent feature of myeloma is its pronounced genetic instability, which is more reminiscent of solid tumors than of hematologic malignancies. Cytogenetic and molecular changes are already present at the premalignant stages, i.e., MGUS and smoldering myeloma (Kyle and Rajkumar, 2006), and increase with conversion to myeloma (Iida and Ueda, 2003), indicating that genomic instability is an early hallmark in myeloma genesis. Aneuploidy and CIN have also been associated with acquired or intrinsic drug resistance (Kops et al., 2005).

(B and C) Overexpression of NEK2 into cancer cell lines and normal cells increased cell proliferation in normal and cancer cells. All results were expressed as means ± SD of three independent experiments.
(D) The cancer cells were fed with medium with or without bortezomib, doxorubicin, and etoposide in plates with single layer agar cultures. Drug treatments decreased significantly colony efficiency values (shown on the figure) in the control group, but decreased much less in the NEK2 overexpressing group. The assay was done in triplicate and the representative images of colonies of ARP1-EV and ARP1-NEK2 OE were shown (4×). Note: we performed all clonogenic assays at the same time for Figure 6G, so the controls used in this Figure and Figure 6G are the same.
(E) ARP1 EV cells showed the sensitivity to all the anticancer drugs using the standard apoptotic assay, and the right-shifted peak indicates cells undergoing apoptosis. More apoptotic cells were seen, associated with a greater shift to the right when higher drug concentrations were applied. The ARP1 cells with NEK2 overexpression showed only a weak right-shifted peak even with high dose treatment.
(F–I) F and H show double stains for CD138 antibody noted as a brown membrane pattern as well as for Ki67 noted as a red nuclear staining pattern using immunohistochemical staining. G and I demonstrate stains for NEK2 with brown nuclear staining pattern. F and G represented one case showing sheets of plasma cells with approximately 5% of CD138 positive plasma cells showing red nuclear staining for Ki-67 (F), while NEK2 was positive in half the cells (G). (H) Neoplastic CD138 positive plasma cells showed 20%–30% positive nuclear staining for Ki67, while (I) these cells were completely negative for NEK2. Note that numerous cells in Figure 3I showed positive nuclear Ki67 staining, but lacked CD138 staining, thus reflecting normal hematopoietic cells. Scale bars, 50 μm.
(J and K) showed double stains for CD138 noted as a red membrane pattern as well as for NEK2 noted as a brown nuclear staining pattern in post-2nd ASCT samples. Scale bars, 50 μm.
See also Figure S2.

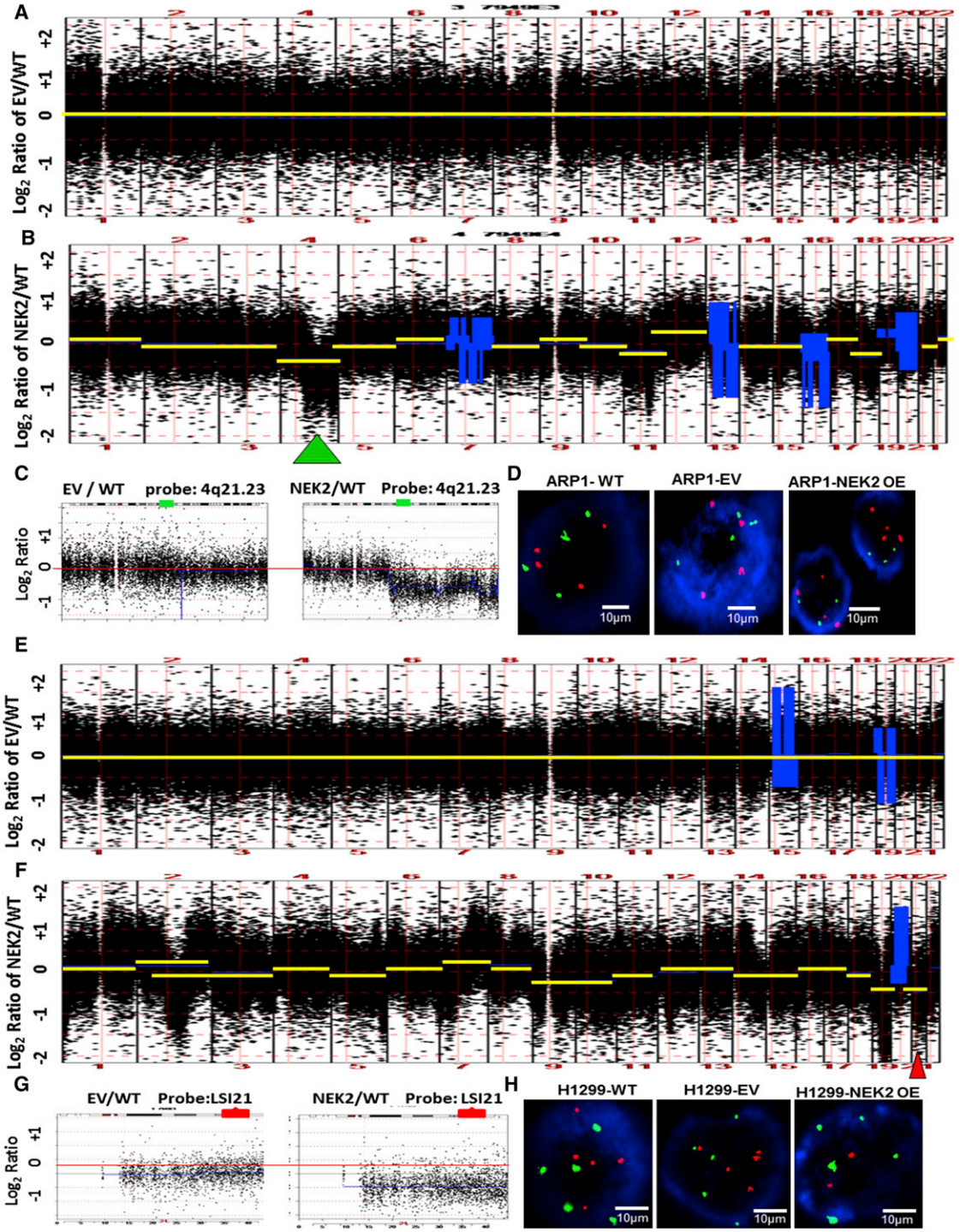

Figure 4. Overexpression of NEK2 Induces Chromosomal Instability

(A, B, E, and F) Array-CGH showed that genome-wide gains and losses in ARP1 (A and B) and H1299 (E and F) cells transfected with EV versus parental (WT) (A and E) and NEK2 cDNA (NEK2) versus parental (B and F). Dots represent the log2 ratio of the intensities for each CGH microarray probe plotted versus the chromosome position. Yellow lines represented the estimated mean of each segment by DNAcopy.

(C) Magnification of a segment of chromosome 4 showed no gain or loss in ARP1 EV versus WT, but losses in ARP1 NEK2 versus WT.

(D) FISH confirmed the loss of 4q21.23 in the NEK2 overexpressing ARP1 cells (three copies) compared to WT ARP1 cells (four copies) and the ARP1-EV (four copies). The control probe CEP10 (D: orange) showed no difference in any of the three ARP1. Scale bars, 10 μm.

(G) Magnification of a segment of chromosome 21 showed losses in the H1299 transfected with NEK2 cDNA but not in the EV.

(H) FISH confirmed the loss of 21q22 in the NEK2-overexpressing H1299 cells (two copies) compared to the H1299-WT cells (five copies) and the H1299-EV (five copies). The control probe CEP7 (H, green) showed no difference in all three H1299 lines. Scale bars, 10 μm.

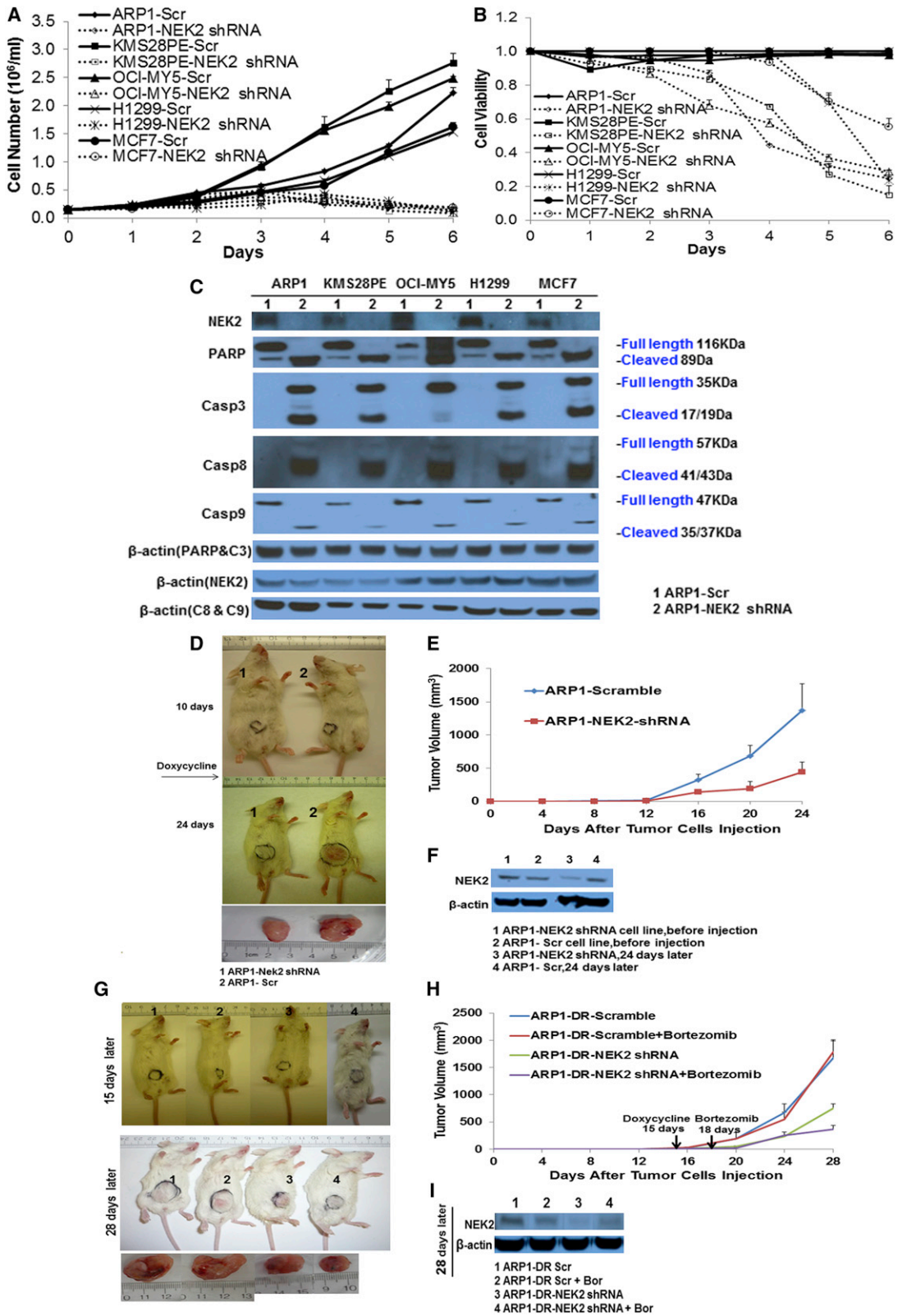

Figure 5. Silencing NEK2 Expression by shRNAs Induces Cancer Cell Growth Inhibition and Decreases Cell Viability

(A and B) 1.5×10^5 cells from the cancer cell lines ARP1, KMS28PE, OCI-MY5, H1299, and MCF7 were transfected with NEK2-shRNA and cultured for 7 days. NEK2-shRNA induced significant growth inhibition (A) and decreased cell viability (B). Cells transfected with scrambled (SCR) sequence served as control; results were expressed as means ± SD of three independent experiments.

(legend continued on next page)

In this study, we discovered that at least two pathways, PP1/AKT and Wnt signaling, are involved in *NEK2*-induced cancer cell drug resistance. It has been revealed that PP1 regulates the AKT signaling pathway to control cell survival and differentiation (Xiao et al., 2010). AKT activation is achieved through a series of phosphorylation steps, the first and the most important step is the phosphorylation at Thr-450, followed by the phosphorylation at Thr-308 and Ser-473 to achieve its full activation (Nicholson and Anderson, 2002). PP1 is a major phosphatase that directly dephosphorylates AKT at Thr-450 to modulate its activation. Our results show that NEK2 binds directly to and phosphorylates PP1 on Thr-320, which results in the upregulation of phosphorylated AKT at Ser-473. ABC transporter family members, *ABCB1*, *ABCC1*, and *ABCG2* are known to play a crucial role in the development of multidrug resistance (Choi, 2005). The ABC transporters colocalize with and can be activated by direct phosphorylation of PIM1 (Xie et al., 2008). Our findings support those of others that *NEK2* stimulates the expression of ABC transporters by activation of AKT and its downstream targets PIM1 and NF-κB, resulting in drug resistance of cancer cells (Misra et al., 2005; Kuo et al., 2002).

AKT plays a central role in cell proliferation (Brunet et al., 1999). AKT also suppresses the pro-apoptotic function of *BCL2* family member *BAD* (Datta et al., 1997) and *BAX* (Gardai et al., 2004). AKT functions through Ikk to promote the transactivation potential and phosphorylation of nuclear factor-κB (NF-κB) (Dan et al., 2008), which activates transcription of pro-survival gene members of the *BCL2* family (*BCL2*, *BCL-xL*, and *MCL1*) (Huang, 2000). In this study, we show clearly that *NEK2* induces the expression of pro-survival genes, while inhibiting pro-apoptotic genes; the AKT inhibitor LY294002 decreases NEK2-induced colony formation, strongly suggesting that *NEK2* induces cell proliferation through AKT signaling.

In the cytoplasm, APC, glycogen synthase kinase-3 (GSK-3) and AXIN form a β-catenin destruction complex which mediates the degradation of β-catenin (Bienz, 2002). Activation of AKT by high expression of NEK2 phosphorylates and deactivates GSK-3 resulting in activation of β-catenin (Monick et al., 2001). Both MAD2 and BubR1 can bind to CDC20 independently and inhibit the activation of APC. Loss of APC or GSK-3 function leads to cytoplasmic β-catenin accumulation and stabilization with constitutive activation of the canonical Wnt signaling pathway (Fodde and Tomlinson, 2010). When cytoplasmic β-catenin is stabilized, it translocates into the nucleus, where it interacts with a family of T cell factor/lymphocyte enhancer factor (TCF-LEF) transcription factors to drive cell proliferation by direct induction of cell cycle regulators, such as *c-Myc* and *cyclin D1* (Gehrke et al., 2009). The TCF/β-catenin complex also regulates ABCB1 by transactivation resulting in drug resistance (Yamada et al., 2000). Knockdown of β-catenin in the ARP1 cell line abrogates NEK2- induced colony formation and drug resistance indicating that β-catenin plays indeed an important role in *NEK2* function.

Although we found that mitotic checkpoint protein MAD2 was upregulated by NEK2, the involvement of this protein on either PP1/AKT or Wnt signaling or both pathways and the role of the checkpoint proteins in *NEK2* induced cancer cell drug resistance and proliferation still needs to be clarified. However, we have demonstrated that NEK2 regulates MAD2, which is also essential spindle checkpoint proteins (Shannon et al., 2002), MAD2 together with BubR1 transmit a "wait signal" and block progression into anaphase until all chromosomes have completely aligned at the metaphase plate (Lee et al., 2004). MAD2 and CDC20 bind directly to NEK2, and CDC20 overexpression is a central feature of the CIN signature (Carter et al., 2006). We found that *NEK2* induces loss of expression of the tumor suppressor gene *APC*. Loss of *APC* function induces CIN seen in many cancers (Rusan and Peifer, 2008). In addition, β-catenin binds to NEK2 at the centrosome and is a key regulator of mitotic centrosome separation (Bahmanyar et al., 2008).

In summary, both PP1/AKT and Wnt pathways are involved in NEK2-induced cancer cell drug resistance, proliferation, and chromosomal instability. Activation of Wnt signaling induced by NEK2 depends partially on the AKT pathway (Figure 7). Downregulation of NEK2 by shRNA inhibited myeloma cell growth and decreased drug resistance in vitro and in NOD-Rag/null gamma mice. Thus, targeting CIN genes, such as NEK2, has the potential to eradicate drug-resistant cells when applied in conjunction with other effective treatments. We are now exploring how NEK2 regulates its downstream targets and how interaction among those pathways is regulated by NEK2.

EXPERIMENTAL PROCEDURES

Study Subjects

Nineteen patients with primary MM including 59 samples at baseline, after chemotherapy (pre-first, pre-second, and post-second ASCTs) were obtained from Huntsman Cancer Institute, University of Utah according to the protocol 25009. Samples for immunohistochemistry (IHC) staining were obtained from the University of Utah and ARUP Institute according to the protocol 40253. Studies are approved by the Institutional Review Board of the University of Utah. Informed consent was obtained in accordance with the Declaration of Helsinki.

(C) Western blots confirmed that NEK2 expression was dramatically decreased in ARP1, KMS28PE, OCI-MY5, H1299, and MCF7 cancer cells transfected with NEK2 shRNA. Silencing NEK2 induced apoptosis through both death receptor-dependent (caspase 8) and -independent (caspase 9) pathways compared with SCR controls.

(D) ARP1 cells were transduced with NEK2 shRNA and SCR control vectors and then injected subcutaneously into the right abdomen of NOD-Rag/null gamma mice. Viral expression was induced by the addition of doxycycline to the drinking water about 10 days after injection of tumor cells. Differences in tumor size are shown between the two groups of mice 24 days after injection of ARP1 cells and 14 days after the addition of doxycycline.

(E) Tumor volume assessments showed that mice with NEK2-shRNA had smaller tumors than the control group.

(F) Western blots showed decreased NEK2 expression in ARP1 cells after NEK2 shRNA activation (number 3).

(G) In the ARP1-DR mice, the groups of 1 to 4 are the group of control (Scr), Scr+ bortezomib, NEK2-shRNA, and NEK2-shRNA + bortezomib, respectively.

(H) Tumor volume assessments showed smaller tumor sizes in NEK2 shRNA-treated mice than in other groups.

(I) Western blots showed decreased NEK2 expression in ARP1-DR cells after NEK2 shRNA activation (groups 3 and 4).

See also Figure S3.

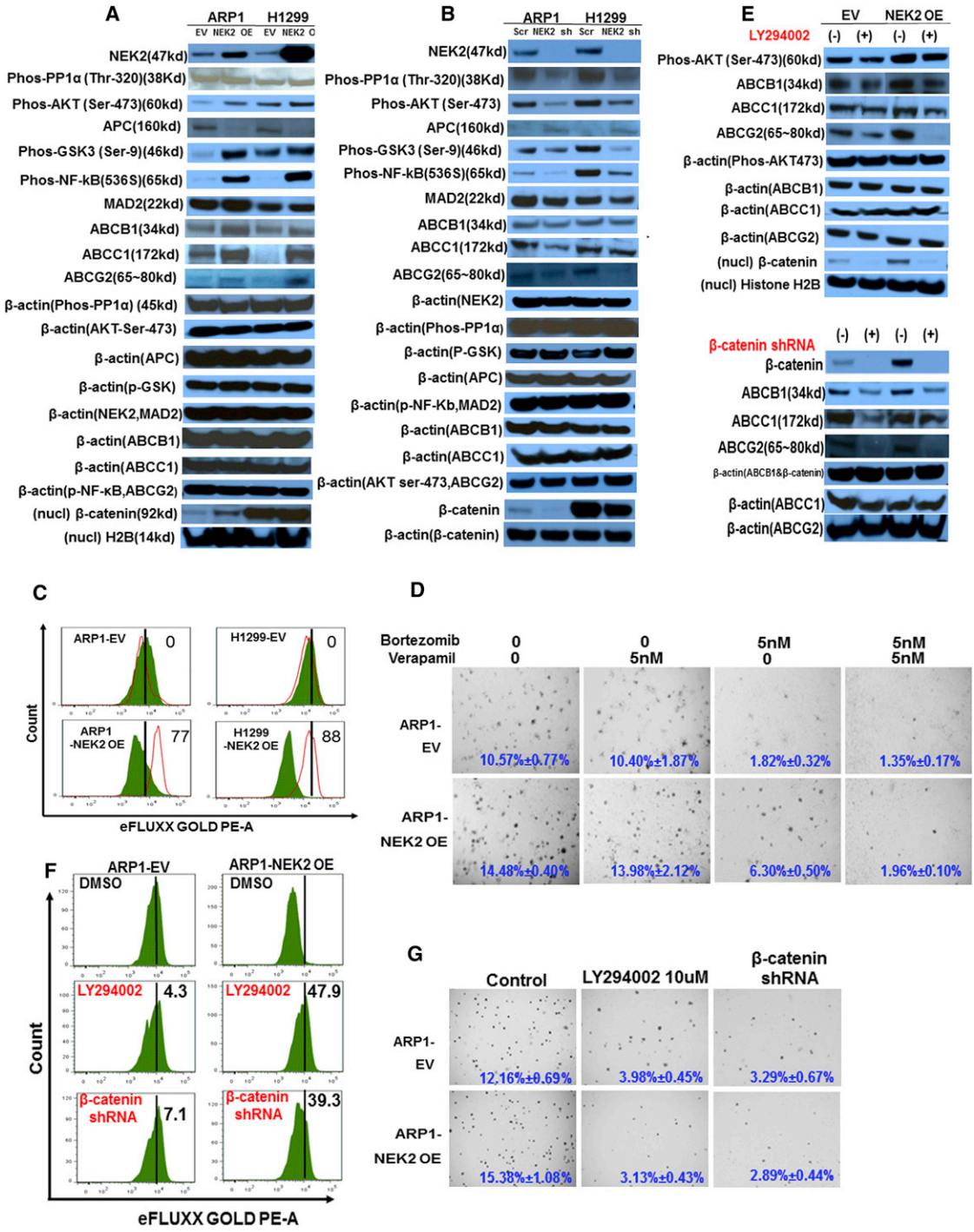

Figure 6. Overexpression of NEK2 Activates both the AKT and Canonical Wnt Signaling Pathways Resulting in Cancer Cell Proliferation, Drug Resistance and Chromosomal Instability

(A) ARP1 and H1299 were transduced with either NEK2 cDNA or EV using a lentiviral delivery system. Increased expression of phos-PP1 and phos-AKT (Ser-473), phos-GSK3, phos-NF-kB, MAD2, ABC transporter members (ABCB1, ABCC1, and ABCG2), and nuclear accumulation of β-catenin was observed on western blotting. We also observed that NEK2 induced decreased expression of APC.

(B) Western blots showed that knockdown NEK2 by shRNA inhibited the activity of AKT and Wnt signaling and decreased the expression of the ABC transporter members in ARP1 and H1299 cells.

(C) Flow cytometry showed that ARP1 and H1299 cells overexpressing NEK2 have a higher efflux of the hydrophilic eFluxx-ID gold fluorescent dye indicating a high activity of ABC transporters in these cells. The ABCB1 or ABCC1 inhibitor increased significantly fluorescent dye in ARP1 and H1299 overexpressed NEK2, respectively ($p < 0.05$). Green tinted and red frame histograms showed fluorescence of pre- and post-inhibitor-treated samples, respectively.

(legend continued on next page)

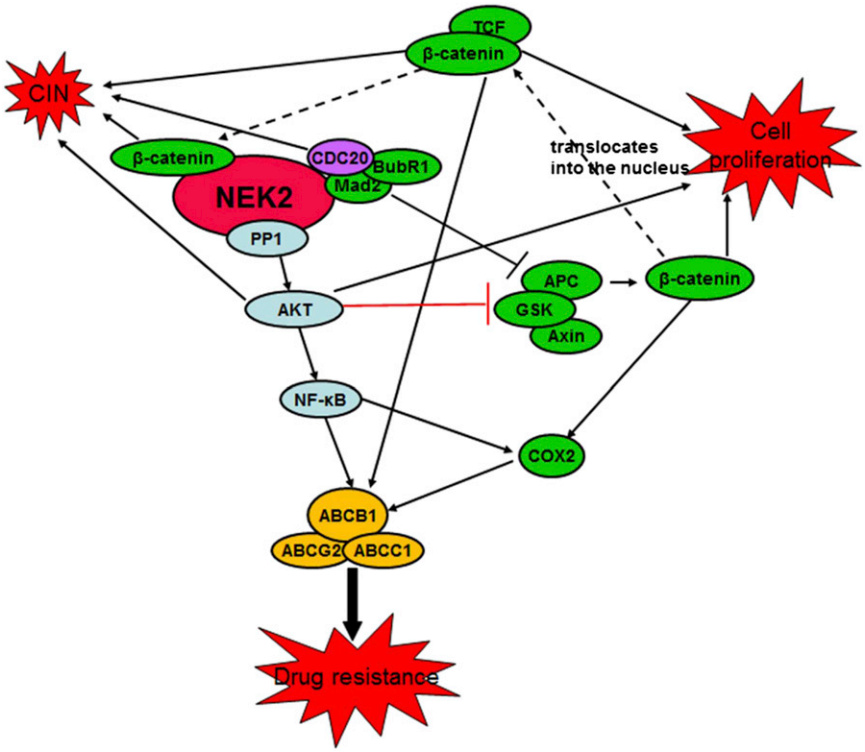

Figure 7. The Model of Our Working Hypothesis

Both PP1/AKT and Wnt pathways are involved in NEK2 inducing cancer cell drug resistance, proliferation, and chromosomal instability.

Plasma cell purifications and GEP and data analysis, using the Affymetrix U133Plus2.0 microarray, were performed as previously described (Zhan et al., 2006), and also described in the Supplemental Information.

Array-CGH Data Analysis

Array-CGH data from the Agilent 180,000-feature human CGH microarray was screened for quality using the Agilent-provided quality control metrics. All arrays passed all ten quality metrics, with signal-to-noise ratios between 72 and 102 (minimum acceptable is 30), and derivative log ratio spread values between 0.14 and 0.17 (maximum acceptable is 0.30). The data were normalized and segmented in R using both the DNAcopy module (Seshan and Olshen, 2010) and the snap CGH package (Smith et al., 2009). The resulting segments were merged with the merge States function (Fridlyand et al., 2004) which combines adjacent segments with similar log ratios. Segments containing at least two microarray probes with $\log_2$ ratios outside the range [−0.3, +0.3] were considered significant.

NOD-Rag/Null Gamma Mice Model of Human Myeloma

All animal work was performed in accordance with the guidelines of the Institutional Animal Care and local veterinary office and ethics committee of the University of Utah, USA (IACUC 08-05004) under approved protocol. ARP1 and ARP1-DR cells were transduced with shRNA and scrambled (SCR) control vectors. 1.5×10^6 cells (in 100 μl PBS) were injected subcutaneously into the abdomen of NOD-Rag/null gamma mice. Tumor burdens were monitored by tumor volumes. Viral expression was induced by the addition of doxycycline (2 mg/ml) to the drinking water (contains 5% sucrose) ~ 10–15 days after injection of tumor cells.

Soft Agar Clonogenic Assay and Standard Apoptosis Assay

Ten thousand cancer cells per well were seeded in 12-well plate for layer agar cultures and treated by multiple drugs at different doses for 3 weeks. Cells were re-suspended in 0.33% agar in MyeloCult H5100 cultures /10% FBS. Cells were fed twice a week by placing two drops of medium on the layer with or without drugs. All plates were taken the photos under microscope, and colony number in the photo was scanned and counted by the ImageJ. The colony efficiency was calculated as (colony number in the photo) × (well area) / (actual area the photo represent) /10,000 × 100%.

For the standard apoptosis assay, all procedures were followed the standard protocol (Annexin V Apoptosis Detection Kit APC, eBioscience). Cells undergoing apoptosis were fixed and the fluorochrome-conjugated Annexin-V was used to visualize the early stage of apoptotic cells and analyzed by flow cytometry.

IHC Staining

Microarray slides were cut at 4 microns on plus slides. Slides are allowed to air dry. Slides were placed in a 55°C–60°C oven for 30 min. The IHC stains were performed on the Ventana automated immunostainer at 37°C (XT/ULTRA, Ventana Medical Systems, Tucson, AZ). Please see details in the Supplemental Experimental Procedures.

FISH

FISH was performed on interphase nuclei using standard methods (Xiong et al., 2008). FISH probes included RP11-397K17 (4q21.23), LSI CEP 10 (control), RUNX1 (21q22), and LSI CEP 7 (control).

Direct Dye Efflux Assay for Multidrug Resistance

The direct dye efflux for multidrug resistance assay was performed essentially as described in the manufacturer's instructions (eFluxx-ID Multidrug resistance assay kits, Enzo Life Sciences, USA). 0.35–0.5 × 10^6 cells were incubated with Gold detection reagent with and without specific inhibitors of ABCB1, ABCC1, and ABCG2 according to the kit protocol for 30 min in 37°C water bath. Cells were suspended in cold PBS for flow cytometry analysis. The MCF7 cells served as a positive control. The formula of calculation

(D) The clonogenic assay showed that the ABC transporter inhibitor verapamil (5 nM) did not inhibit colony formation in both EV and NEK2 OE ARP1 cells. Bortezomib treatment decreased colony efficiency values shown on the figure in the ARP1 EV group, but much less in the NEK2 OE group. The combination of verapamil and bortezomib showed a significant decrease of colony efficiency value in ARP1 NEK2-OE cells (4×).
(E) Western blots showed that the AKT inhibitor LY294002 at a dose of 10 μM for 12 hr (top panel) and β-catenin shRNA (bottom panel) inhibited the expression of the ABC transporter members ABCB1, ABCC1 and ABCG2 in both EV and NEK2 OE cells, and LY294002 also decreased the nuclear accumulation of β-catenin (top panel).
(F) Inhibition of AKT and Wnt signaling decreased the efflux of the hydrophilic eFluxx-ID gold fluorescent dye showing increased significantly fluorescent dye in ARP1-NEK2 OE cells treated with LY294002 or β-catenin shRNA ($p < 0.05$). The MAF is shown in the figure.
(G) The clonogenic assay showed that both LY294002 and β-catenin shRNA treatments significantly inhibited colony formation in both EV and NEK2 OE cells ($p < 0.01$), especially in the latter (4×).
The same membrane was reprobed for the internal control of β-actin or histone H2B for western blot in (A), (B), and (E). See also Figure S4 and Table S2.

of multidrug resistance activity factor (MAF) is described in the instruction of the MDR assay kit.

Statistical Analysis

All data were shown as means ± SD. The Student's t test was used to compare two experimental groups. In correlation of *NEK2* expression with disease progression, event-free and OSs were measured using the Kaplan-Meier method, and the log-rank test was used for group comparison. Significance was set at $p < 0.05$.

ACCESSION NUMBERS

The Gene Expression Omnibus database accession number for the microarrays performed on primary myeloma sequential samples reported in this paper is GSE19554.

SUPPLEMENTAL INFORMATION

Supplemental Information includes two tables, four figures, and Supplemental Experimental Procedures and can be found with this article online at http://dx.doi.org/10.1016/j.ccr.2012.12.001.

ACKNOWLEDGMENTS

This work was supported by National Cancer Institute grants R01CA115399 (to G.T.), R01CA152105 (to F.Z.), and R21CA143887 (to F.Z.), the MMRF Senior (to F.Z., 2008 and 2010), the leukemia lymphoma society TRP (to F.Z., 2010 and 2011), and institutional start -up funds from the School of Medicine and Huntsman Cancer Institute of the University of Utah (to F.Z.).

Received: November 14, 2010
Revised: March 22, 2011
Accepted: December 4, 2012
Published: January 14, 2013

REFERENCES

Avet-Loiseau, H., Facon, T., Grosbois, B., Magrangeas, F., Rapp, M.J., Harousseau, J.L., Minvielle, S., and Bataille, R.; Intergroupe Francophone du Myélome (2002). Oncogenesis of multiple myeloma: 14q32 and 13q chromosomal abnormalities are not randomly distributed, but correlate with natural history, immunological features, and clinical presentation. Blood *99*, 2185–2191.

Bahmanyar, S., Kaplan, D.D., Deluca, J.G., Giddings, T.H., Jr., O'Toole, E.T., Winey, M., Salmon, E.D., Casey, P.J., Nelson, W.J., and Barth, A.I. (2008). beta-Catenin is a Nek2 substrate involved in centrosome separation. Genes Dev. *22*, 91–105.

Barlogie, B., Tricot, G., Anaissie, E., Shaughnessy, J., Rasmussen, E., van Rhee, F., Fassas, A., Zangari, M., Hollmig, K., Pineda-Roman, M., et al. (2006). Thalidomide and hematopoietic-cell transplantation for multiple myeloma. N. Engl. J. Med. *354*, 1021–1030.

Bergsagel, P.L., Kuehl, W.M., Zhan, F., Sawyer, J., Barlogie, B., and Shaughnessy, J., Jr. (2005). Cyclin D dysregulation: an early and unifying pathogenic event in multiple myeloma. Blood *106*, 296–303.

Bienz, M. (2002). The subcellular destinations of APC proteins. Nat. Rev. Mol. Cell Biol. *3*, 328–338.

Brunet, A., Bonni, A., Zigmond, M.J., Lin, M.Z., Juo, P., Hu, L.S., Anderson, M.J., Arden, K.C., Blenis, J., and Greenberg, M.E. (1999). Akt promotes cell survival by phosphorylating and inhibiting a Forkhead transcription factor. Cell *96*, 857–868.

Calasanz, M.J., Cigudosa, J.C., Odero, M.D., Ferreira, C., Ardanaz, M.T., Fraile, A., Carrasco, J.L., Solé, F., Cuesta, B., and Gullón, A. (1997). Cytogenetic analysis of 280 patients with multiple myeloma and related disorders: primary breakpoints and clinical correlations. Genes Chromosomes Cancer *18*, 84–93.

Carter, S.L., Eklund, A.C., Kohane, I.S., Harris, L.N., and Szallasi, Z. (2006). A signature of chromosomal instability inferred from gene expression profiles predicts clinical outcome in multiple human cancers. Nat. Genet. *38*, 1043–1048.

Choi, C.H. (2005). ABC transporters as multidrug resistance mechanisms and the development of chemosensitizers for their reversal. Cancer Cell Int. *5*, 30.

Dan, H.C., Cooper, M.J., Cogswell, P.C., Duncan, J.A., Ting, J.P.Y., and Baldwin, A.S. (2008). Akt-dependent regulation of NF-kappaB is controlled by mTOR and Raptor in association with IKK. Genes Dev. *22*, 1490–1500.

Datta, S.R., Dudek, H., Tao, X., Masters, S., Fu, H., Gotoh, Y., and Greenberg, M.E. (1997). Akt phosphorylation of BAD couples survival signals to the cell-intrinsic death machinery. Cell *91*, 231–241.

Faragher, A.J., and Fry, A.M. (2003). Nek2A kinase stimulates centrosome disjunction and is required for formation of bipolar mitotic spindles. Mol. Biol. Cell *14*, 2876–2889.

Fodde, R., and Tomlinson, I. (2010). Nuclear beta-catenin expression and Wnt signalling: in defence of the dogma. J. Pathol. *221*, 239–241.

Fridlyand, J., Snijders, A., Pinkel, D., Albertson, D., and Jain, A. (2004). Application of Hidden Markov Models to the analysis of the array CGH data. J. Multivariate Anal. *90*, 132–153.

Fry, A.M., Mayor, T., Meraldi, P., Stierhof, Y.D., Tanaka, K., and Nigg, E.A. (1998). C-Nap1, a novel centrosomal coiled-coil protein and candidate substrate of the cell cycle-regulated protein kinase Nek2. J. Cell Biol. *141*, 1563–1574.

Fu, G., Ding, X., Yuan, K., Aikhionbare, F., Yao, J., Cai, X., Jiang, K., and Yao, X. (2007). Phosphorylation of human Sgo1 by NEK2A is essential for chromosome congression in mitosis. Cell Res. *17*, 608–618.

Gardai, S.J., Hildeman, D.A., Frankel, S.K., Whitlock, B.B., Frasch, S.C., Borregaard, N., Marrack, P., Bratton, D.L., and Henson, P.M. (2004). Phosphorylation of Bax Ser184 by Akt regulates its activity and apoptosis in neutrophils. J. Biol. Chem. *279*, 21085–21095.

Gehrke, I., Gandhirajan, R.K., and Kreuzer, K.A. (2009). Targeting the WNT/beta-catenin/TCF/LEF1 axis in solid and haematological cancers: Multiplicity of therapeutic options. Eur. J. Cancer *45*, 2759–2767.

Hayward, D.G., and Fry, A.M. (2006). Nek2 kinase in chromosome instability and cancer. Cancer Lett. *237*, 155–166.

Helps, N.R., Luo, X., Barker, H.M., and Cohen, P.T. (2000). NIMA-related kinase 2 (Nek2), a cell-cycle-regulated protein kinase localized to centrosomes, is complexed to protein phosphatase 1. Biochem. J. *349*, 509–518.

Hose, D., Rème, T., Hielscher, T., Moreaux, J., Messner, T., Seckinger, A., Benner, A., Shaughnessy, J.D., Jr., Barlogie, B., Zhou, Y., et al. (2011). Proliferation is a central independent prognostic factor and target for personalized and risk-adapted treatment in multiple myeloma. Haematologica *96*, 87–95.

Huang, Z. (2000). Bcl-2 family proteins as targets for anticancer drug design. Oncogene *19*, 6627–6631.

Iida, S., and Ueda, R. (2003). Multistep tumorigenesis of multiple myeloma: its molecular delineation. Int. J. Hematol. *77*, 207–212.

Jemal, A., Siegel, R., Ward, E., Hao, Y., Xu, J., and Thun, M.J. (2009). Cancer statistics, 2009. CA Cancer J. Clin. *59*, 225–249.

Kops, G.J., Weaver, B.A., and Cleveland, D.W. (2005). On the road to cancer: aneuploidy and the mitotic checkpoint. Nat. Rev. Cancer *5*, 773–785.

Kuo, M.T., Liu, Z., Wei, Y., Lin-Lee, Y.C., Tatebe, S., Mills, G.B., and Unate, H. (2002). Induction of human MDR1 gene expression by 2-acetylaminofluorene is mediated by effectors of the phosphoinositide 3-kinase pathway that activate NF-kappaB signaling. Oncogene *21*, 1945–1954.

Kwon, Y.G., Lee, S.Y., Choi, Y., Greengard, P., and Nairn, A.C. (1997). Cell cycle-dependent phosphorylation of mammalian protein phosphatase 1 by cdc2 kinase. Proc. Natl. Acad. Sci. USA *94*, 2168–2173.

Kyle, R.A., and Rajkumar, S.V. (2006). Monoclonal gammopathy of undetermined significance. Br. J. Haematol. *134*, 573–589.

Lee, E.A., Keutmann, M.K., Dowling, M.L., Harris, E., Chan, G., and Kao, G.D. (2004). Inactivation of the mitotic checkpoint as a determinant of the efficacy of

microtubule-targeted drugs in killing human cancer cells. Mol. Cancer Ther. *3*, 661–669.

Misra, S., Ghatak, S., and Toole, B.P. (2005). Regulation of MDR1 expression and drug resistance by a positive feedback loop involving hyaluronan, phosphoinositide 3-kinase, and ErbB2. J. Biol. Chem. *280*, 20310–20315.

Monick, M.M., Carter, A.B., Robeff, P.K., Flaherty, D.M., Peterson, M.W., and Hunninghake, G.W. (2001). Lipopolysaccharide activates Akt in human alveolar macrophages resulting in nuclear accumulation and transcriptional activity of beta-catenin. J. Immunol. *166*, 4713–4720.

Moreau, P., Facon, T., Leleu, X., Morineau, N., Huyghe, P., Harousseau, J.L., Bataille, R., and Avet-Loiseau, H.; Intergroupe Francophone du Myélome (2002). Recurrent 14q32 translocations determine the prognosis of multiple myeloma, especially in patients receiving intensive chemotherapy. Blood *100*, 1579–1583.

Morris, N.R. (1975). Mitotic mutants of Aspergillus nidulans. Genet. Res. *26*, 237–254.

Nicholson, K.M., and Anderson, N.G. (2002). The protein kinase B/Akt signalling pathway in human malignancy. Cell. Signal. *14*, 381–395.

Oakley, B.R., and Morris, N.R. (1983). A mutation in Aspergillus nidulans that blocks the transition from interphase to prophase. J. Cell Biol. *96*, 1155–1158.

Rusan, N.M., and Peifer, M. (2008). Original CIN: reviewing roles for APC in chromosome instability. J. Cell Biol. *181*, 719–726.

Seshan, V., and Olshen, A. (2010). DNAcopy: DNA copy number data analysis. R package version 1.20.0. (Seattle, WA: Bioconductor).

Shannon, K.B., Canman, J.C., and Salmon, E.D. (2002). Mad2 and BubR1 function in a single checkpoint pathway that responds to a loss of tension. Mol. Biol. Cell *13*, 3706–3719.

Shaughnessy, J.D., Jr., Zhan, F., Burington, B.E., Huang, Y., Colla, S., Hanamura, I., Stewart, J.P., Kordsmeier, B., Randolph, C., Williams, D.R., et al. (2007). A validated gene expression model of high-risk multiple myeloma is defined by deregulated expression of genes mapping to chromosome 1. Blood *109*, 2276–2284.

Shipp, M.A., Ross, K.N., Tamayo, P., Weng, A.P., Kutok, J.L., Aguiar, R.C., Gaasenbeek, M., Angelo, M., Reich, M., Pinkus, G.S., et al. (2002). Diffuse large B-cell lymphoma outcome prediction by gene-expression profiling and supervised machine learning. Nat. Med. *8*, 68–74.

Smith, M., Marioni, J., Hardcastle, T., and Thorne, N. (2009). snapCGH: Segmentation, Normalization and Processing of aCGH Data Users' Guide. Bioinformatics *22*, 1144–1146.

Sonn, S., Jeong, Y., and Rhee, K. (2009). Nip2/centrobin may be a substrate of Nek2 that is required for proper spindle assembly during mitosis in early mouse embryos. Mol. Reprod. Dev. *76*, 587–592.

Storchova, Z., and Kuffer, C. (2008). The consequences of tetraploidy and aneuploidy. J. Cell Sci. *121*, 3859–3866.

Wu, L., Osmani, S.A., and Mirabito, P.M. (1998). A role for NIMA in the nuclear localization of cyclin B in Aspergillus nidulans. J. Cell Biol. *141*, 1575–1587.

Xiao, L., Gong, L.L., Yuan, D., Deng, M., Zeng, X.M., Chen, L.L., Zhang, L., Yan, Q., Liu, J.P., Hu, X.H., et al. (2010). Protein phosphatase-1 regulates Akt1 signal transduction pathway to control gene expression, cell survival and differentiation. Cell Death Differ. *17*, 1448–1462.

Xie, Y., Xu, K., Linn, D.E., Yang, X., Guo, Z., Shimelis, H., Nakanishi, T., Ross, D.D., Chen, H., Fazli, L., et al. (2008). The 44-kDa Pim-1 kinase phosphorylates BCRP/ABCG2 and thereby promotes its multimerization and drug-resistant activity in human prostate cancer cells. J. Biol. Chem. *283*, 3349–3356.

Xiong, W., Wu, X., Starnes, S., Johnson, S.K., Haessler, J., Wang, S., Chen, L., Barlogie, B., Shaughnessy, J.D., Jr., and Zhan, F. (2008). An analysis of the clinical and biologic significance of TP53 loss and the identification of potential novel transcriptional targets of TP53 in multiple myeloma. Blood *112*, 4235–4246.

Yamada, T., Takaoka, A.S., Naishiro, Y., Hayashi, R., Maruyama, K., Maesawa, C., Ochiai, A., and Hirohashi, S. (2000). Transactivation of the multidrug resistance 1 gene by T-cell factor 4/beta-catenin complex in early colorectal carcinogenesis. Cancer Res. *60*, 4761–4766.

Zhan, F., Huang, Y., Colla, S., Stewart, J.P., Hanamura, I., Gupta, S., Epstein, J., Yaccoby, S., Sawyer, J., Burington, B., et al. (2006). The molecular classification of multiple myeloma. Blood *108*, 2020–2028.